FEBS Letters 390 (1996) 280–284 FEBS 17283

Do voltage-gated Kv1.1 and inward rectifier Kir2.1 potassium channels form heteromultimers?

Jan Tytgat[a,b,*], Gunnar Buyse[b], Jan Eggermont[b], Guy Droogmans[b], Bernd Nilius[b], Paul Daenens[a]

[a] *University of Leuven, Laboratory of Toxicology, Van Evenstraat 4, B-3000 Leuven, Belgium*
[b] *University of Leuven, Laboratory of Physiology, Campus Gasthuisberg, O & N, B-3000 Leuven, Belgium*

Received 11 April 1996; revised version received 23 May 1996

Abstract Possible heteromultimer formation between Kv- and Kir-type K^+ channels was investigated, in connection with the known functional diversity of K^+ channels in vivo. Voltage-clamp experiments were performed on *Xenopus* oocytes, either injected with concatenated Kir2.1-Kv1.1 mRNA, or co-injected with Kv1.1 and Kir2.1 mRNA. K^+ currents could be approximated by the algebraic sum of the 2 K^+ current types alone. The tandem construct did not show functional expression, although it could be detected by Western blotting. We conclude that Kv1.1 and Kir2.1 α-subunit proteins fail to assemble and do not contribute functional diversity to K^+ channels.

Key words: Potassium channel; Ion channel; α-Subunit; Oocyte

1. Introduction

Functional diversity of voltage-gated K^+ channels can be attributed to the presence of many Kv gene products [1], but also to the possibility of heteromultimerization of the α-subunit proteins within, but not among, the *Shaker*, *Shab*, *Shaw* and *Shal* subfamilies [2–5]. When expressed in *Xenopus* oocytes or transfected cells, Kv channel polypeptides assemble to form tetramers [6,7]. The basis for the incompatibility among subfamilies is the sequence contained within the T1 assembly or tetramerization domain [8]. Expression cloning of inwardly rectifying K^+ channel (Kir) cDNAs [9–11] and subsequent homology screening [12] have revealed a novel family of mammalian K^+ channel genes that encode proteins with structural and functional features distinct from the Kv channel superfamily. Evidence for heteromultimer formation between two distinct inwardly rectifying K^+ channel subunits, GIRK1 (Kir3.1) and CIR (Kir3.4), has recently been published [13]. However, the molecular rules for subunit co-assembly remain largely unknown [14], as there are only two reports on the analysis of subunit assembly of Kir channels. Based on the differential sensitivity to voltage-dependent block by spermine, there is evidence that functional Kir channel proteins are also composed of four subunits [15]. Using an alternative approach, the tetrameric stoichiometry of Kir channels was determined by linking together the coding sequence of three or four IRK1 subunits [16], a procedure successfully applied by us to determine the stoichiometry of Kv channels [7].

The assumption that functional diversity of K^+ channels can also be attributed to possible heteromultimerization between Kv-type and Kir-type channels has, to our knowledge, never been verified. We have therefore investigated if Kv1.1 α-subunits can co-assemble with Kir2.1 subunits to produce functional channels by expressing a tandem channel composed of Kir2.1 and Kv1.1, and by performing co-injection experiments in *Xenopus* oocytes. As prototype channels for the Kv1.1 and Kir2.1 family, we have used the RCK1 clone [17] and the IRK1 clone [9], respectively.

2. Materials and methods

2.1. Construction of IRK1/pGEMHE2 and of the tandem channel

The IRK1 cDNA clone in its original vector, pcDNA1/Amp (Invitrogen, USA), was first subcloned into a custom-made high expression vector, pGEMHE [7], by digestion of IRK1/pcDNA1/Amp with *Not*I restriction endonuclease (New England Biolabs, USA) and blunting the cohesive ends with DNA polymerase I (large Klenow fragment). Next this linearized cDNA was digested with *Bam*HI and the 5.4 kb IRK1-containing fragment was genecleaned for ligation. The pGEMHE vector was digested with *Xba*I, followed by blunting its cohesive ends with DNA polymerase I (large Klenow fragment). Next this linearized DNA was also digested with *Bam*HI and the 3 kb pGEMHE-containing fragment was genecleaned for ligation with the IRK1 fragment. The ligation product, IRK1/pGEMHE, was again subcloned into another custom-made high-expression vector, pGEMHE2. This was done by digestion of IRK1/pGEMHE and the original vector pGEMHE with *Bam*HI and *Nhe*I. A small, genecleaned fragment of 1.8 kb coding for the entire IRK1 channel was then ligated with a 2.8 kb fragment from the vector. The ligation product, IRK1/pGEMHE2, was verified with restriction digests *Nhe*I, *Bam*HI + *Nhe*I and *Pst*I.

The tandem channel was constructed by digestion of IRK1/pGEMHE2 and RKC1/pGEMHE (as described in [7]) with *Bsa*BI, using SCS110 cells (Stratagene, USA) for transformation because of dam/dcm methylation. The linearized fragments of ~4.6 kb containing the IRK1 and RCK1 cDNA were then genecleaned and treated with *Xma*I. The IRK1 cDNA was then inserted as a 1.1 kb fragment into the 4.4 kb RCK1/pGEMHE construct. The ligation product, IRK1/RCK1/pGEMHE, was verified with *Pst*I, *Bam*HI and *Hin*dIII and is called hereafter 'tandem' channel, with the coding sequences of both channel types in one open reading frame. After translation of the corresponding mRNA, residue Asp-249 in the C-terminus of the IRK1 channel is covalently linked to residue Ile-43 in the N-terminus of the RCK1 channel, which is illustrated in Fig. 1.

2.2. Expression in oocytes

For in vitro transcription, plasmids were first linearized either with *Nhe*I (for IRK1/pGEMHE2), or with *Pst*I 3′ to the 3′ non-translated β-globin sequence of RCK1/pGEMHE and IRK1/RKC1/pGEMHE. Next the 'Riboprobe Gemini System' was used (Promega, USA) with T7 RNA polymerase and a cap analogue diguanosine triphosphate. Isolation of *Xenopus laevis* oocytes was as previously described [7]. mRNA was injected at a concentration of 5 ng/50 nl for RCK1, IRK1 and the tandem construct, and 2.5 ng/50 nl for RCK1 and IRK1 in the co-injection experiments. For each channel construct, at least two independent clones were transcribed, injected and expressed.

*Corresponding author. Fax: (32) (16) 32-34-05.
E-mail: jan.tytgat@med.kuleuven.ac.be

PII S0014-5793(96)00674-6

2.3. Electrophysiological recordings and analysis

Whole-cell currents from oocytes were recorded using the two-microelectrode voltage-clamp technique (GeneClamp 500, Axon Instruments, USA). Resistances of voltage and current electrodes were kept as low as possible (0.2–1 MΩ) and were filled with 3 M KCl or 1 M K_3citrate plus 10 mM KCl. Current records were sampled at 1 ms intervals and filtered at 0.5 kHz, using a 4-pole low-pass Bessel filter. To eliminate the effect of the voltage drop across the bath grounding electrode, the bath potential was actively controlled. Capacitative and leak currents were not subtracted. All experiments were performed at room temperature (19–23°C) and constant perfusion rate (2.5 ml/min).

2.4. Immunoblotting

Translational efficacy of heterologous RCK1 and tandem proteins in *Xenopus laevis* oocytes was checked by immunoblotting 150 μg of soluble protein extract with affinity-purified polyclonal anti-RCK1 antibodies [18]. 48 h after injection, defolliculated native and injected oocytes were lysed in a hypotonic buffer (see Section 2.5). The lysate was centrifuged and the supernatant stored at −20°C. Protein concentration was determined by the enhanced protocol of the bicinchoninic acid method of Pierce (Rockford, USA) using bovine serum albumin as a standard. 150 μg of protein extracts were separated on SDS-PAGE (10% polyacrylamide) and transferred to a 0.45 μm nitrocellulose membrane (Hybond-ECL, Amersham, USA) by semi-dry electroblotting. After serial incubation with affinity-purified rabbit polyclonal anti-RCK1 antiserum in a 1:100 dilution and peroxidase labeled anti-rabbit immunoglobulins (Amersham, USA) diluted 1:1000 respectively, RCK1 and tandem proteins were detected using chemoluminescence (Amersham, USA).

2.5. Solutions

The ND-96 solution contained (in mM): 96 NaCl, 2 KCl, 1.8 $CaCl_2$, 1 $MgCl_2$, 5 HEPES, pH 7.5, supplemented with 50 mg/ml gentamicin sulfate (only for incubation). Voltage-clamp experiments were performed in the original or modified ND-96 solution, containing either 2, 3, 4 or 98 mM external [K^+] with the external [NaCl+KCl] = 98 mM. The hypotonic buffer for lysis contained (in mM): 20 NaCl, 2.5 EGTA, 25 Tris, pH 7.5, supplemented with Nonidet P-40 0.5% (v/v).

3. Results

In a first series of protocols, hyperpolarizing and depolarizing test pulses (V_{test}) ranging from −160 to +60 mV from a holding potential (V_{hold}) of 0 mV were applied every 5 s to *Xenopus* oocytes injected with mRNA coding either for IRK1, RCK1, IRK1+RCK1 (='co-injection'), or the 'tandem' channel (Fig. 2). The channel encoded by the IRK1 cDNA clone is an authentic inward rectifier K^+ channel, because of its ability to pass large inward K^+ currents below E_K (observed reversal potential, E_{rev}, ∼−84 mV) as compared to minimal outward K^+ currents. This feature is illustrated in the current/voltage relationship (*I/V*) in the presence of 4 mM extracellular [K^+] (Fig. 2B). The channel encoded by the RCK1 cDNA clone is inactivated at V_{hold} 0 mV and therefore, no time-dependent currents are present during V_{test} from −160 to +60 mV. In contrast, large slowly inactivating outward tail currents were observed at V_{hold} 0 mV, as the channels recovered from inactivation during the preceding V_{test}. The extent of recovery was thereby proportional to the extent of hyperpolarization. By plotting the amplitude of the tail currents as a function of the preceding V_{test}, a typical inactivation curve for RCK1 was obtained (Fig. 2B, open circles). Co-injection of the IRK1 and RCK1 cDNA clones resulted in K^+-selective currents with large inward currents below E_K and slowly inactivating outward tail currents. The kinetics and voltage dependence of these currents are proportionally not different from the sum of the two native channels and, hence, do not support heteromultimer formation between the two channel types. Oocytes injected with our concatenated construct, characterized by two pore domains in tandem, did not reveal functional expression when clamping from V_{hold} 0 mV to V_{test} −160 to +60 mV.

In a second series of protocols, depolarizing test pulses ranging from −80 to +30 mV from a holding potential of −90 mV were applied every 5 s in the presence of 4 mM extracellular [K^+] (Fig. 3). The holding current at −90 mV evoked by the IRK1 clone was inward, confirming the observed E_{rev} ∼−84 mV in the *I/V* relationship in Fig. 2B. During V_{test}, no substantial time-dependent K^+ currents were present. However at V_{hold} −90 mV, the inward tail currents inactivated slowly with kinetics reminiscent of IRK1 activation when stepping from V_{hold} 0 mV to V_{test} −90 mV [9]. Depolarization of oocytes expressing the RKC1 clone resulted in fast activating and not or slowly inactivating (delayed rectifier) K^+ currents. The corresponding macroscopic *I/V* plot illustrates the outwardly rectifying behavior of RKC1, in contrast to IRK1. Tail currents were absent at V_{hold} −90 mV, because of the very fast deactivation process of RCK1 at −90 mV and of V_{hold} close to E_K [19]. Co-injection of the IRK1 and RCK1 cDNA clones resulted in K^+-selective currents with an outward component positive to −30 mV carried by RCK1 channels, and a slowly inactivating in-

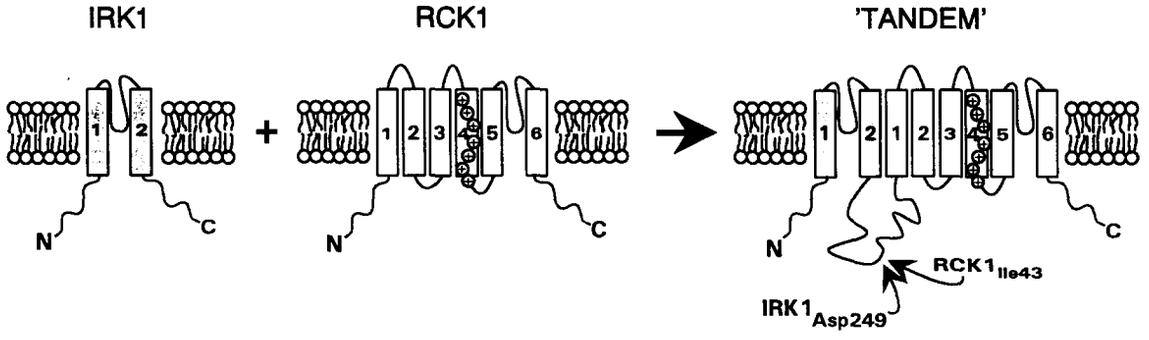

Fig. 1. Postulated transmembrane orientation of IRK1, RCK1 and the 'TANDEM' construct. The IRK1 channel (with 2 transmembrane regions, M1 and M2, flanking the pore region) was covalently linked to the RKC1 channel (with 6 transmembrane regions, S1 to S6, and the pore region residing between S5 and S6) by concatenating residue Asp-249 in the C-terminus of the IRK1 channel to residue Ile-43 in the N-terminus of the RCK1 channel. The resulting heterodimer contains the coding sequences of both channel types in one open reading frame with their two pore regions in 'tandem'.

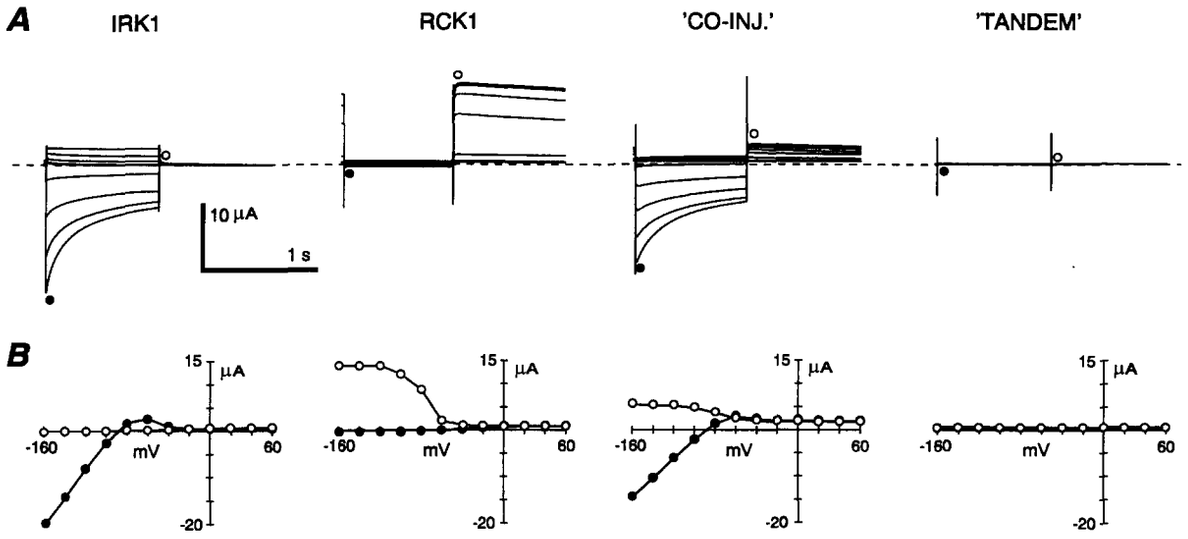

Fig. 2. Macroscopic currents in *Xenopus laevis* oocytes from V_{hold} 0 mV. A: Current recordings obtained with the two-microelectrode voltage-clamp technique in the presence of 4 mM extracellular [K^+]. Oocytes were held at V_{hold} 0 mV and stepped every 5 s to V_{test} +60 to −160 mV for 1 s. Oocytes co-injected with IRK1 and RCK1 mRNA ('CO-INJ.') displayed K^+-selective currents which were proportionally not different from the sum of IRK1 and RCK1. The 'TANDEM' construct did not reveal functional expression. B: *I/V* relationships corresponding to the currents shown in panel A, with peak currents (filled circles) evoked during V_{test} values. The observed E_{rev} ∼−87 mV, close to E_K = −84 mV as predicted by the Nernst equation. Peak tail currents (open circles) measured at V_{hold} 0 mV are plotted as a function of the preceding V_{test} values, resulting in a typical inactivation curve for RCK1.

ward tail current component carried by IRK1 channels. The kinetics and voltage dependence of these currents are again proportionally not different from the sum of the two native channels. Oocytes injected with the tandem channel did not reveal functional expression.

In an effort to rescue our concatenated channel construct, with two pores in tandem, we also performed experiments in a bath solution containing an elevated external [K^+] of 98 mM. The reasoning behind was that we might have 'missed' functional expression in low external [K^+], because at all tested voltages either the IRK1 pore in the tandem was 'open' (i.e. not blocked by Mg or polyamines), or the RKC1 pore was 'open' (i.e. channel not in the resting or inactivated state), but the two pores were never 'open' in tandem at the same time. By raising the extracellular [K^+] to 98 mM, the voltage ranges at which the pores of both the IRK1 and RCK1 channel part are 'open' for the permeation of K^+ ions would now coincide. In spite of this approach with 98 mM extracellular [K^+], the tandem channel still failed to yield functional currents when the same two voltage protocols as before were applied (Fig. 4). In contrast, the RCK1 clone produced voltage- and time-dependent K^+ currents, with characteristics typically seen in elevated external [K^+] conditions: an inward K^+ current component below the E_{rev} value of ∼−3 mV and inward fast

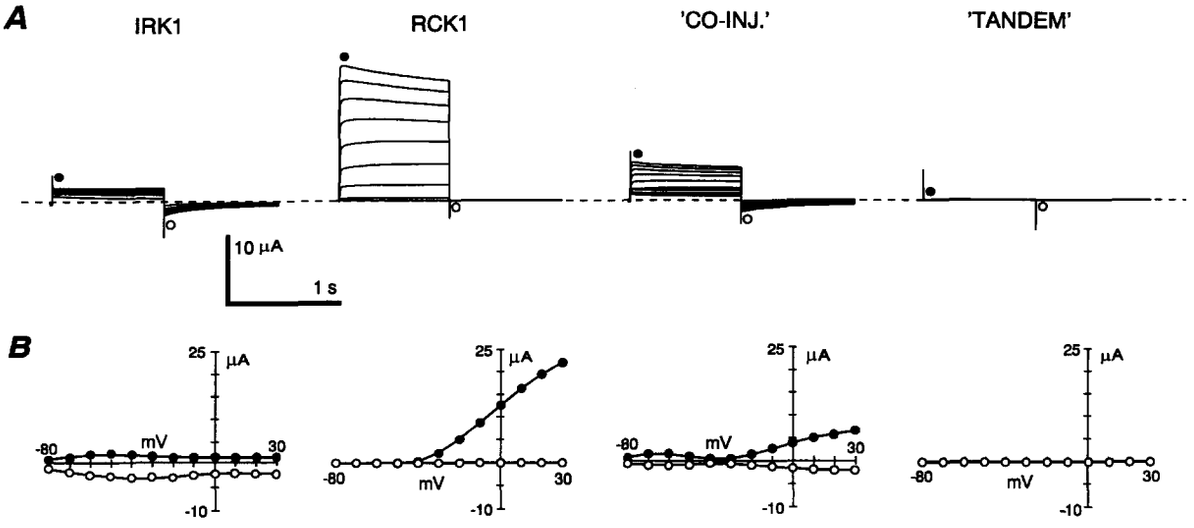

Fig. 3. Macroscopic currents in *Xenopus laevis* oocytes from V_{hold} −90 mV. A: Oocytes were clamped at V_{hold} −90 mV and stepped every 5 s to V_{test} ranging from −80 to +30 mV for 1 s in the presence of 4 mM extracellular [K^+]. Co-injected oocytes ('CO-INJ.') displayed K^+-selective currents which were proportionally not different from the sum of IRK1 and RCK1. The 'TANDEM' construct did not reveal functional expression. B: *I/V* relationships corresponding to the currents shown in panel A, with peak currents (filled circles) evoked during V_{test} values and peak tail currents (open circles) during V_{hold} plotted as a function of the preceding V_{test} values.

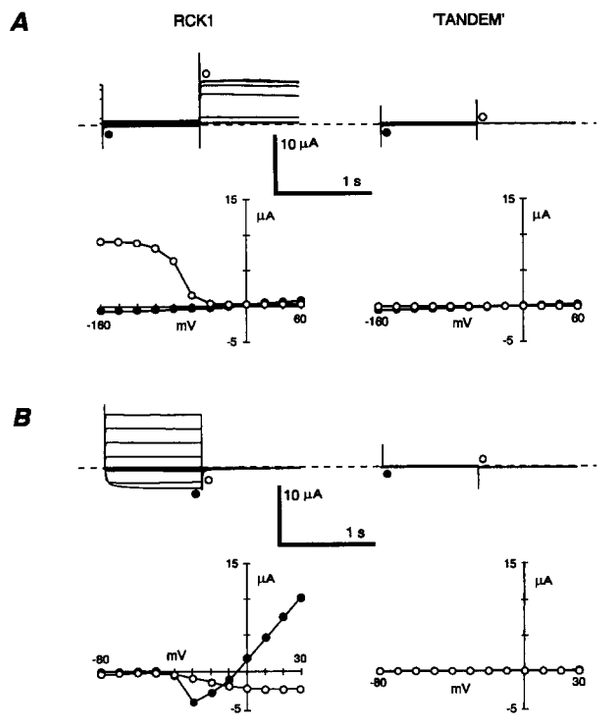

Fig. 4. Macroscopic currents in *Xenopus laevis* oocytes in the presence of 98 mM extracellular [K^+]. A: Macroscopic currents with corresponding *I/V* relationships below as obtained by clamping from V_{hold} 0 mV to V_{test} ranging from +60 to −160 mV for 1 s in duration at a frequency of 0.2 Hz. The 'TANDEM' channel did not reveal functional expression. Peak currents evoked during V_{test} (filled circles); peak tail currents during V_{hold} plotted as a function of the preceding V_{test} (open circles). B: Macroscopic currents with corresponding *I/V* relationships below as obtained by clamping from V_{hold} −90 mV to V_{test} ranging from −80 to +30 mV for 1 s in duration at a frequency of 0.2 Hz. The 'TANDEM' channel did not reveal functional expression. Peak currents evoked during V_{test} (filled circles); peak tail currents during V_{hold} plotted as a function of the preceding V_{test} (open circles).

inactivating tail currents at V_{hold} −90 mV (Fig. 4B). Because of the large inward currents (> 50 μA) evoked at hyperpolarized potentials (−160 to −100 mV) in the presence of 98 mM external [K^+], no reliable voltage clamps could be obtained for oocytes injected with the IRK1 clone as well as for the co-injected oocytes (data not shown).

Since we did not see any functional expression with the tandem channel, we were interested in the translational efficacy of the heterologous tandem protein, and of the RCK1 protein for comparison, in *Xenopus laevis* oocytes. This was checked by immunoblotting 150 μg of soluble protein extracts with affinity-purified polyclonal anti-RCK1 antibodies [18], 48 h after injection of the oocytes. A representative Western blot containing soluble protein extracts of defolliculated native (non-injected), RCK1-injected and tandem-injected oocytes is shown in Fig. 5. Anti-RCK1 antiserum intensely labeled a band of the protein extract, obtained from oocytes injected with the RCK1 clone, with a molecular weight of ~61 kDa. This value is larger than the molecular mass predicted from its nucleotide sequence (56.4 kDa), but corresponds fairly well to the size of the Kv1.1 channel protein (~59 kDa) synthesized in a microsome-containing in vitro translation extract [20]. Anti-RCK1 antiserum also intensely labeled a larger band of the protein extract, now obtained from oocytes injected with the tandem construct, with a molecular weight of ~76 kDa. This value approximates the predicted molecular mass (79.9 kDa) of the tandem construct. As the polyclonal antibodies are specific for the C-terminal region of the RCK1 channel, and thus also for the C-terminus of our tandem construct, the intense labeling of a ~76 kDa band indicates that the mRNA coding for our tandem channel is translated efficaciously.

4. Discussion

We report here that RCK1 and IRK1 α-subunits fail to assemble into heteromultimers and do not contribute functional diversity to K^+ channels. In contrast, evidence for heteromultimer formation within, but not among, certain Kv and Kir subfamilies has been documented [2–5,13,21]. In connection with structural diversity of K^+ channels, two new classes represented by respectively TOK1 and YKC1 isolated from *Saccharomyces cerevisiae*, and CeK1,2,3 from the nematode *Caenorhabditis elegans*, have recently been reported [22–24]. It has been proposed that these channels, characterized by the unique feature of two pore domain-containing subunits in tandem, may function as a dimer. The TOK1 and YKC1 channels exhibit an outwardly rectifying K^+ selective current, with a conduction-voltage relationship sensitive to extracellular K^+ concentration [22,23]. These attributes are similar to those described for Kir channels, but in the opposite direction. Interestingly, the hydropathy profile of TOK1 and YKC1 is reminiscent of a Kv-like channel attached to a Kir-like channel, with the first pore domain located between S5 and S6, and the second positioned between S7 and S8. The stoichiometry, membrane topology and possible subunit co-assembly of the TOK1 and YKC1 protein, as well as of CeK1, CeK2, and CeK3, however, remain to be established. Different from these channel proteins, our data do not suggest dimer formation between RCK1 and IRK1 α-subunit proteins. However, we cannot generalize our findings and exclude that other members of Kv and Kir channels do not oligomerize as well. Furthermore, it has to be noticed that our concatenated construct with two pore domains in tandem has the two pore regions separated by four transmembrane segments, whereas the TOK1 and YKC1 protein have flanking pore domains. Given that the K^+ currents seen in the co-injection experiments could be approximated by the algebraic sum of RCK1 and IRK1 K^+ current types, and hence that there is no evidence for heteromultimerization, it is not very likely that a dimeric construct, where now the carboxy-terminal end of RCK1 is linked to the amino terminus of IRK1, will give rise to outwardly rectifying K^+ currents.

Although our tandem construct did not reveal functional expression in oocytes, it could be labeled by Western blotting using an affinity-purified rabbit polyclonal anti-RCK1 antiserum. The detection of a band with a molecular mass of ~76 kDa by the antiserum specific for the C-terminal region of the RCK1 protein indicates that the translation of the entire tandem protein has occurred properly and does not explain the lack of functional expression. There are, however, several possibilities for the lack of functional expression, like deficient transport to the cell membrane or improper folding in the cell membrane. One conclusion we can draw from our tandem construct is that concatenating IRK1 to RCK1 prevents either channel type from functioning.

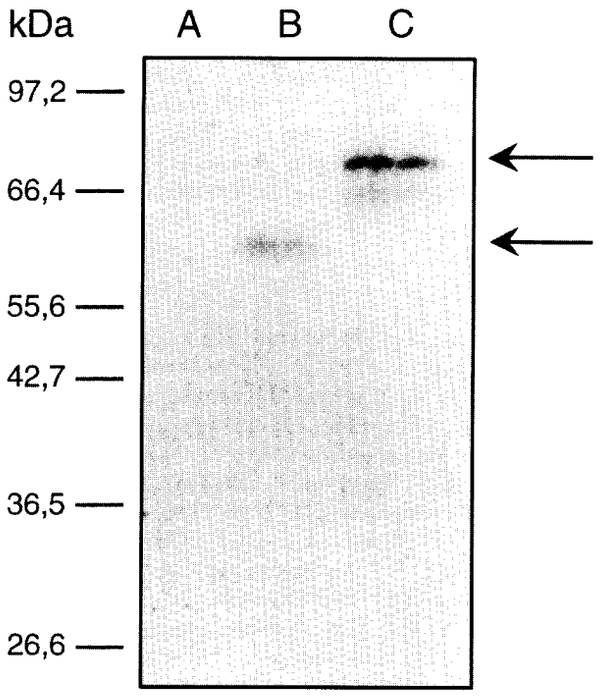

Fig. 5. Heterologous expression of RCK1 and 'TANDEM' construct in *Xenopus laevis* oocytes. A Western blot containing soluble protein extracts (150 μg per lane) of defolliculated native (A), RCK1-injected (B) and 'TANDEM'-injected (C) oocytes was incubated with affinity-purified rabbit polyclonal anti-RCK1 antiserum and subsequently stained by chemoluminescence. In lane B, RCK1 migrates as a 61 kDa protein (predicted molecular mass is 56.4 kDa). The 'TANDEM' construct migrates as a 76 kDa protein in lane C (predicted molecular mass is 79.9 kDa).

As our data are from whole-cell recordings, the lack of any perceptible outward tail current in IRK1 at V_{test} positive to E_K (Fig. 2) is most likely caused by extrinsic cytoplasmic polyamine blockers [14]. Assuming a K^+-selective channel, the observed E_{rev} value of ~ -84 mV in the presence of 4 mM extracellular $[K^+]$ and the observed E_{rev} value of ~ -3 mV in 98 mM extracellular $[K^+]$ indicates that the intracellular $[K^+]$ of the oocytes is ~ 110 mM, which is slightly higher than the 90 mM reported by Dascal [25]. The fact that no time-dependent RCK1 current is observed during V_{test} (Fig. 2) is owing to the prolonged depolarization at V_{hold} 0 mV during which RCK1 inactivates slowly. This phenomenon was originally described by Nakajima et al. for I_K in many cell types [26].

Acknowledgements: The IRK1 cDNA clone was kindly provided by L.Y. Jan. Polyclonal anti-RCK1 antibodies were kindly provided by S. Sewing. Gunnar Buyse is a Research Assistant of the Nationaal Fonds voor Wetenschappelijk Onderzoek (N.F.W.O., Belgium). Jan Eggermont and Jan Tytgat are Research Associates of the N.F.W.O. (Belgium).

References

[1] Strong, M., Chandy, K.G. and Gutman, G.A. (1993) Mol. Biol. Evol. 10, 221–242.
[2] Christie, M.J., North, R.A., Osborne, P.B., Douglass, J. and Adelman, J.P. (1990) Science 244, 221–224.
[3] Isacoff, E.Y., Jan, Y.N. and Jan, L.Y. (1990) Nature 345, 530–534.
[4] Ruppersberg, J.P., Schroter, K.H., Sakmann, B., Stocker, M., Sewing, S. and Pongs, O. (1990) Nature 345, 535–537.
[5] McCormack, K., Lin, W., Iverson, L.E. and Rudy, B. (1990) Biochem. Biophys. Res. Commun. 171, 1361–1371.
[6] Mackinnon, R. (1991) Nature 350, 232–235.
[7] Liman, E.R., Tytgat, J. and Hess, P. (1992) Neuron 9, 861–871.
[8] Shen, N.V. and Pfaffinger, P.J. (1995) Neuron 14, 625–633.
[9] Kubo, Y., Baldwin, T.J., Jan, Y.N. and Jan, L.Y. (1993) Nature 362, 127–133.
[10] Ho, K., Nichols, C.G., Lederer, W.J., Lytton, J., Vassilev, P.M., Kanazirska, M.V. and Hebert, S.C. (1993) Nature 362, 31–38.
[11] Dascal, N., Schreibmayer, W., Lim, N.F., Wang, W., Chavkin, C., Dimagno, L., Labarca, C., Kieffer, B.L., Gaveriaux-Ruff, C., Trollinger, D., Lester, H.A. and Davidson, N. (1993) Proc. Natl. Acad. Sci. USA 90, 10235–10239.
[12] Kubo, Y., Reuveny, E., Slesinger, P.A., Jan, Y.N. and Jan, L.Y. (1993) Nature 364, 802–806.
[13] Krapivinsky, G., Gordon, E.A., Wickman, K., Velimirovic, B., Krapivinsky, L. and Clapham, D.E. (1995) Nature 374, 135–141.
[14] Doupnik, C.A., Davidson, N. and Lester, H.A. (1995) Curr. Opin. Neurobiol. 5, 268–277.
[15] Glowatzki, E., Fakler, G., Brändle, U., Rexhausen, U., Zenner, H.-P., Ruppersberg, J.P. and Fakler, B. (1995) Proc. R. Soc. Lond. B 261, 251–261.
[16] Yang, J., Jan, Y.N. and Jan, L.Y. (1995) Neuron 15, 1441–1447.
[17] Baumann, A., Grupe, A., Ackermann, A. and Pongs, O. (1988) EMBO J. 7, 2457–2463.
[18] Scott, V.E.S., Muniz, Z.M., Sewing, S., Lichtinghagen, R., Parcej, D.N., Pongs, O. and Dolly, J.O. (1994) Biochemistry 33, 1617–1623.
[19] Koren, G., Liman, E.R., Logothetis, D.E., Nadal-Ginard, B. and Hess, P. (1990) Neuron 4, 39–51.
[20] Deal, K.K., Lovinger, D.M. and Tamkun, M.M. (1994) J. Neurosci. 14, 1666–1676.
[21] Covarrubias, M., Wei, A. and Salkoff, L. (1991) Neuron 7, 763–773.
[22] Ketchum, K.A., Joiner, W.J., Sellers, A.J., Kaczmarek, L.K. and Goldstein, S.A.N. (1995) Nature 376, 690–695.
[23] Zhou, X.-L., Vaillant, B., Loukin, S.H., Kung, C. And Saimi, Y. (1995) FEBS Lett. 373, 170–176.
[24] Salkoff, L. and Jegla, T. (1995) Neuron 15, 489–492.
[25] Dascal, N. (1987) Crit. Rev. Biochem. 22, 317–387.
[26] Nakajima, S., Iwasake, S. and Obata, K. (1962) J. Gen. Physiol. 46, 97–115.